Design of a TV White Space Converter Prototype Towards Cognitive Radio for WLAN Routers

I. Subbiah*, M. Schrey*, A. Ashok*, G. Varga*, A. Achtzehn†, M. Petrova†, and S. Heinen*
*Chair of Integrated Analog Circuits and RF Systems
Email: {isubbiah, mschrey, ashok, gvarga, heinen}@ias.rwth-aachen.de
†Institute for Networked Systems
Email: {aac, mpe}@inets.rwth-aachen.de
RWTH Aachen University, D-52062 Aachen, Germany

***Abstract*—We report on the development of a frequency converter frontend that enables 2.4 GHz IEEE 802.11 WLAN devices to operate in unused parts of the UHF spectrum, the so-called TV whitespaces. The new frontend features separate TX and RX paths with automatic directionality switching and in-hardware energy detection. Equipped with a standard antenna port at the input side, and a fully configurable transmit chain controlled through a user-accessible microcontroller, this whitespace converter (WSC) with commercial off-the-shelf components is particularly suitable for cognitive radio (CR) research. We discuss the specific challenges in the design of a WSC for 802.11 WLAN routers. The complete architecture is presented, and preliminary performance results from a level plan optimization are discussed.**

I. Introduction

The realization of the next generation of high-data rate wireless networks will, without doubt, depend on the amount of available spectrum. The rapid growth of the number of wireless devices that overwhelm the networks with traffic and the growing dependency of society on fast and reliable wireless Internet access motivate predictions of an upcoming spectrum shortage. Several measurement campaigns have revealed that many licensed frequency bands are potentially underutilized [1]. In order to enable efficient usage of spectrum, spectrum-agile cognitive radio (CR) techniques and spectrum re-farming approaches have been proposed to enable reuse of licensed spectrum on an opportunistic basis by secondary users [2]. Due to their favorable propagation characteristics, the UHF bands currently reserved for TV broadcasting have drawn a lot of attention as potentially attractive bands for implementation of new secondary radio technologies. These so-called *TV whitespaces (TVWS)* are currently both spatially and temporally underutilized in many regulatory domains.

After the initial rulemaking by FCC [3] allowing secondary use in the US, trials are currently underway which quantify the prospects of TVWS operations. In order to minimize radio overhead and cut manufacturing costs, and given that most personal communication devices like smartphones or tablets are already equipped with multi-band transceivers, e.g. IEEE 802.11 WLAN, the possibilities of enabling legacy technologies to use additional bands seem highly sensible. However, previous studies for selected broadcasting regions have shown though, that practical spectrum availability and power constraints may effectively limit the benefits of using secondary devices in the TVWS [4]. Even further complexity arises from the tough requirements a CR transceiver frontend needs to meet in order to comply with today's stringent specifications of diverse communication standards [5]. In this paper we study the design challenges of extending existing WLAN transceivers for TVWS operations by means of implementing a flexible and generic *whitespace converter (WSC)*. Particularly we address the complexity issue of this essential part of CR technologies. Our WSC acts as a bidirectional frequency converter that shifts WLAN radio operations to the TVWS.

The developed WSC aims to simplify comparison studies and directly enable experimental CR research. Whereas earlier ISM-UHF converters such as [6] united TX and RX paths and allowed only coarse-grained control of the whitespace operation parameters, our design separates the paths and thereby enables individual on-the-fly reconfiguration of key TX/RX chain parameters, e.g. gain and synthesizer settings. Furthermore we support in-hardware energy detection for spectrum sensing without the need for additional signal processor. The developed WSC can be connected to unmodified commercial WLAN equipments such as IEEE 802.11 access points or adapters, thereby easing the deployment of testbeds significantly. This paper provides the design details to the community, and at the time of this writing, a first experimental 'production run' of larger samples for research purposes is already undertaken.

The focus of this paper is to give an overview and initial performance assessment of our WSC design. We identify the specific requirements imposed by the stringent specifications of the legacy IEEE 802.11 standard and show how they have been met in the selection of components and hardware layout. The rest of the paper is organized as follows: In Section II we discuss objectives and technology-specific challenges for an ISM-UHF converter platform. Section III describes the overall architecture of our novel WSC design with separate TX and RX paths. In Section IV we identify relevant performance metrics and present our findings from an initial optimization study. Section V concludes the paper.

II. Design Objectives and Challenges

We will start by briefly discussing the main design targets of a WSC and the challenges imposed on it by IEEE legacy standards and operational environment. The purpose of the WSC design is to provide an easy-to-use, yet flexible platform for extending IEEE 802.11 devices with CR functionalities, and to enable them to access local TVWS spectrum resources. In order to achieve compatibility with a variety of commercial IEEE 802.11 hardware, direct access to baseband signals seems improbable, hence the WSC is required to shift signals from the 2.4 GHz ISM band that are accessible at the antenna output to the UHF bands. Because of the differences in the regional regulatory constraints, the device needs to be able to support different legacy WLAN output powers and UHF output powers. Furthermore, whereas our current focus is on the support of IEEE 802.11 b/g [7], [8] devices with channel bandwidths of 22 MHz and 20 MHz respectively, we aim for a wide 80 MHz sub-band for the frequency conversion. This will allow studies of fast adaptive channel usage without need for slow WSC synthesizer recalibration. The device needs to be fully configurable, i.e. key parameters of the transceiver will need to be adjustable on the fly. Since only few routers allow to run a custom firmware, the control needs to be out-of-band through separate signalling.

We foresee several challenges that may arise from the high signal purity requirements of IEEE 802.11 devices, since the WSCs at transmitter and receiver side increase the unwanted distortions and noise levels. First, the allowable interference from a TVWS link conversion must be minimized, in order to stay within the limits of the standards' specification. This becomes particularly difficult because of the signal impurities from both the WSC and the original WLAN transceiver chain, that need to be compensated for. For low-quality WLAN adapters, we presume this will grant only a small error budget, thus the WSC must be of considerably high quality.

A second practical issue we identified is the signal power of the incumbent broadcasting networks in channels that are adjacent to the whitespace devices' operation channels. We see a significant threat of frontend desensitization at the WSC if no proper filtering is applied. Due to the fragmentation of channel use in today's broadcasting networks, that becomes particularly apparent in urban regions [9]. Here, TV channels are locally spread throughout the entire UHF spectrum, with only few unused channels in-between them. Tuning the transceiver to channels with high frequency offset from the broadcasting channels may hence be impossible. To minimize harm from the incumbent, a frequency mapping from UHF to ISM band will need to made in such way that the incumbent's signal is outside the passband of a large subset of the in-built filters.

III. WSC Architecture

The architecture of our WSC device is depicted in Fig. 1. The WSC is based on a high-IF transceiver architecture for which unwanted spurious RX band emissions due to the LO harmonics do not pose a problem. Unlike earlier works (e.g., [6]), our transceiver consists of a separate transmit and receive path. This enables us to a more fine-grained configuration of the different components, thereby to optimize independently for transmit signal purity and receiver sensitivity. The two paths are separated and unified with the help of two fast SPDT RF switches, one of which (the IF switch) is located at the IF port facing the WLAN router and the other one (the RF switch) merging the signal paths to allow for single UHF antenna operations.

While most of the signal processing elements are unique to their respective paths, we have opted for a common UHF low pass filter between the antenna port and the RF switch. This LPF combined with the inherent selectivity of the antenna and the LNA's input matching network, forms a bandpass network for the rejection of unwanted interference from the lower-frequency broadcast networks, that may otherwise desensitize the LNA. Also, in the presence of a high power ($>$ -20 dBm) in-band interferer, the LNA can be driven into low gain mode thereby preventing the desensitization of the frontend. In the symmetric transceive path at the input side in between the router RF port and the IF switch, a small portion of the WLAN transmit signal is coupled out and fed into an RF power detector controlling the RF switches. For the purpose of providing optional connectivity for additional measurement equipment, another small portion of the received router signal (6 dB coupling) is fed into a third, auxiliary RF connector.

A. Transmit Path

The transmit path begins after the signal-separating RX and TX switch and has a digital attenuator as the first element of the signal chain. This allows for supporting different router signal strength settings and making tradeoffs between noise and linearity. Additionally, slow power-level control through a microcontroller interface (see below) can be implemented. The attenuator provides up to 31 dB power backoff. All the potential spurs from the WLAN router will be attenuated by the 2.4 GHz ISM bandpass SAW filter which follows the attenuator.

The highly linear downconversion mixer then translates the WLAN signal into the UHF band of our interest using a local oscillator (LO) signal created by the synthesizer. The resulting signal, located in the 470-790 MHz UHF band, is still degraded by inevitable mixer spurs, which are all lying above the wanted signal frequency. Therefore, a UHF low pass filter is necessary to remove these nonlinearities. The power amplifier is capable of 30 dBm output power and the attenuator provides power backoff when needed. This amplified output signal is then fed to the antenna through the RF switch. The whole signal processing path uses single-ended signal transmission.

B. Receive Path

The first stage of our receiver is an LNA that has a high gain of 22 dB and a very low noise figure (NF) of 0.45 dB. The receiver chain exhibits superior noise rejection capabilities as apparent from these key metrics. The upconversion mixer then translates the desired UHF frequencies into the 2.4 GHz ISM

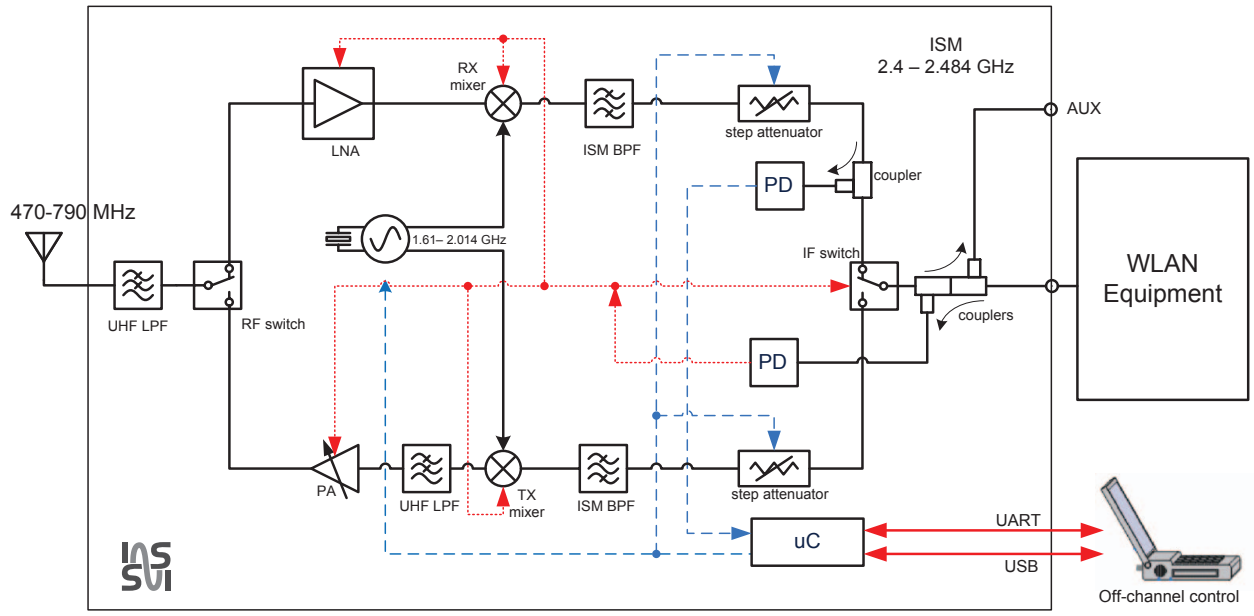

Fig. 1. Complete block diagram of the proposed white space converter.

band. An additional ISM band pass filter removes the spurs generated by the mixer and any other unwanted frequency contents. Since the bandwidth of this band pass filter is 80 MHz, only a small fraction of the UHF band is selected. By tuning the synthesizer, any 80 MHz band within the targeted UHF band can be selected. Through the WLAN device's in-built receiver chain, further channel selection can be done. Due to its attenuation characteristics, the ISM filter can also be used to suppress unwanted signal sources in the incumbent broadcasting networks by translating the desired channels close to the transition band of the ISM filter.

The possibility of widely varying signal strengths is the reason for additionally including a digitally controllable attenuator in the receive path. Here, a power backoff of up to 31 dB can be realized. Since detecting broadcasts or PMSE users does not require baseband decoding, a method of RF power detection is provided in the hardware. This also has the advantage that it can be detected faster in hardware and with few resources. Therefore, the received signal coming from the attenuator is coupled to an RF power detector in front of the RF switch. Like the transmit path, the receive path signal processing section is also entirely single-ended.

C. Synthesizer

The LO consists of a wideband synthesizer chip, an external loop filter for the PLL and an external reference crystal resonator to achieve a carrier signal with the needed phase noise performance. Since the WLAN router operates in TDD mode, both mixers can be operated with the same LO frequency. The loop dynamics of the PLL are tailored to achieve minimum phase noise and thereby maximizing its performance. Furthermore, PLL settings can be selected to comply with the settling time required for spectrum sensing purposes.

D. TX/RX Switching and External Control

The various parts of the signal chain are controlled by two mechanisms. Firstly, the transmit signal from the router is fed to a power detector, which is in controller mode. Hereby, if the input power reaches a predefined threshold, the converter is switched to transmit mode. The shortest preamble of IEEE 802.11 packets is 96 us whereas the switching delay of the RF switch is 150 ns, which is sufficiently short not to incur any information loss. If the power from the router falls below the user-specified threshold, the WSC is returned to receive mode. In either mode, the unused blocks in the other signal path are switched off to conserve power and to reduce local interference.

The second, off-channel control mechanism has been realized through a microcontroller (an ATxMega32 from Atmel). It controls the attenuation settings for both the transmit path and the receive path. The microcontroller also reads the analog voltage from the RF power detector and provides digital readout of this value through both a legacy serial port and a USB port.

IV. System Design for IEEE 802.11 Compliance

Our system implementation has been tailored to the stringent signal purity requirements of IEEE 802.11 devices. This step is not straightforward as the WSC incurs additional noise and distortions beyond those that are already present in the internal 2.4 GHz transceiver chain of the source device. Hence, the demands to preserve operational compliance are comparably strict and lie within the tight boundaries between a vendor design's performance and the compliance limits. In the following, we discuss the level plan of our converter and show how it is optimized between two key performance

TABLE I
BRIEF SUMMARY OF IEEE 802.11 b/g WLAN

Frequency	2.4 - 2.4835 GHz
Bandwidth	22 MHz / 20 MHz
Modulation	DSSS, CCK, BPSK, QPSK, 16-QAM, 64-QAM
Bitrate	1 Mbps to 54 Mbps
Sensitivity	-82 dBm to -65 dBm
TX Power	+20 dBm (Europe); +30 dBm (US)

parameters, namely the Noise Figure (NF) and the Third-Order Input Intercept Point (IIP3).

A. Level Plan

A brief summary of the specifications of the 802.11 b/g [7], [8] standard is shown in Table I. With the requirements laid down by these standards, the system design of the WSC has been carried out with the help of level plan. Any RF transceiver is limited by the lowest and the highest signal levels that it is able to successfully demodulate, i.e. the signal levels at which it achieves demodulation with an acceptable bit error rate (BER). The lowest level is determined by the noise introduced by the receiver chain and the highest tolerable signal level is dictated by the linearity characteristic of the receiver chain. The distribution of the various parameters of the components such as gain, noise figure and IIP3 is accomplished in a level plan in such a way that the noise and linearity of the link comply with the specifications of the communication standard. The level plan of this converter is shown in Fig. 2.

The figure of merit that stands for noise introduced by any component is the noise figure. To begin with, the tolerance margin for the receiver noise figure can be deduced from the standards. The NF of a receiver, expressed in dB, is defined as

$$NF = P_{min} - 10\log(kT) - 10\log B - SNR \qquad (1)$$

where $\mathrm{P_{min}}$ indicates the sensitivity level, i.e. the weakest signal that the receiver should be able to successfully demodulate while still maintaining an acceptable BER. kT is the thermal noise density, B is the bandwidth of the channel and SNR is the required signal-to-noise ratio for any given modulation. The SNR can be further expressed as

$$SNR = \frac{E_b}{N_o} + \eta_{eff}. \qquad (2)$$

Here, SNR is expressed in units of dB, $\mathrm{E_b/N_o}$ is the information-bit-energy to noise-density of the communication expressed in dB and η_{eff} is the spectral efficiency of the modulation system expressed in bps/Hz.

With an example, the NF analysis of our system can be explained. The IEEE 802.11g mode with BPSK modulation that provides a data rate of 6 Mbps can be considered. The sensitivity for this particular mode is stated to be -82 dBm and the channel bandwidth of 802.11g is known to be 20 MHz. The SNR can be neglected by taking into account that the spectral efficiency of BPSK modulation technique for this data rate amounts to 0.36 bps/Hz and $\mathrm{E_b/N_o}$ for the specified bite error rate in 802.11g is required to be better than 10^{-5}. Entering these values into (2), the minimum SNR becomes 6.1 dB. Applying this value into (1), and using the numerical value of the thermal noise density as -174 dBm/Hz, the tolerable noise figure for this data rate is found to be 13.7 dB. Correspondingly, evaluating the tolerable noise figure margin for other data rate modes of 802.11b and 802.11g standard results in various NF values and the worst case among those turns out to be 11.7 dB. In order to operate with a safety margin, a noise figure of less than 8.5 dB is targeted here for the combined architecture of the WSC and the WLAN router.

The figure of merit that attributes the highest signal level tolerable by the receiver is the third order input intercept point (IIP3). The requirement for this IIP3 point is usually specified in standards by a two tone intermodulation test. In this test, the maximum power levels of two interferers with a particular frequency spacing between them are specified. In the presence of such interferers, no deterioration of the performance of the receiver is expected. The IIP3 point is then given by

$$P_{IIP3} = P_{INT} + \frac{(P_{INT} - P_{IMD3})}{2}, \qquad (3)$$

where all the terms are expressed in dBm, $\mathrm{P_{INT}}$ is power level of the interferer and $\mathrm{P_{IMD3}}$ is the level of the intermodulation products generated due to nonlinearities. In order to minimize signal quality degradation due to incumbent transmissions, it is desired that the level of the intermodulation products stays well below the level of the desired frequency signal by a margin larger than the SNR required for the used modulation technique.

In the 802.11 b/g specifications, the intermodulation tests are not mentioned explicitly. However, to arrive at an estimate for the IIP3, the levels of the desired and the unwanted blockers from the adjacent channel selectivity tests need to be taken into account. For example, according to the adjacent channel selectivity test of 802.11b, the receiver should show no performance degradation when an unwanted interferer which is 41 dB above the sensitivity level is being received at 25 MHz away from the desired channel. The level of the desired signal is at -70 dBm and the unwanted interferer is set to -35 dBm. An SNR of 9 dB is required for the 11 Mbps data rate mode to achieve a BER better than 10^{-5}. Substituting these values into (3), the IIP3 point turns out to be -20.5 dBm. A similar analysis for 802.11g leads to an IIP3 point of -56.5 dBm which is not stringent as compared to the 802.11b mode. Additionally, the intermodulation test outlined in the original 802.11 specifications imply an IIP3 point of the receiver to be at -34.5 dBm. As a final target for our implementation, an IIP3 level of better than -15 dBm for the combined setup of the WSC and WLAN router is sought after.

B. Optimization of the Level Plan

Following the component selection, the optimization of the overall converter plus router setup was carried out using the attenuator block. As the attenuator can vary its attenation

Stage #		0	1		2		3		4		5		6		7		8		9	
		Antenna	Switch		UHF Filter		LNA		Mixer		SAW Filter		Attenuator		Coupler		Switch		Coupler	
Power Gain	[dB]		-0.8		-1.4		22.0		3.5		-1.2		-1.0		-1.1		-1.0		-1.5	
Power Gain	-		0.8		0.7		158.5		2.2		0.8		0.8		0.8		0.8		0.7	
Noise Figure	[dB]		0.8		1.4		0.5		12.5		1.2		1.0		1.1		1.0		1.5	
Noise Factor	-		1.2		1.4		1.1		17.8		1.3		1.3		1.3		1.3		1.4	
IIP3	[dBm]		54.0		60.0		12.5		22.0		60.0		52.0		60.0		53.0		60.0	
IIP3	[mW]		inf		inf		17.8		158.5		inf		inf		inf		inf		inf	
Cascaded Gain	[dB]			-0.8		-2.2		19.8		23.3		22.1		21.1		20.0		19.0		17.6
Cascaded Gain	-			0.8		0.6		96.2		215.3		163.3		129.7		100.7		80.0		57.3
Cascaded Noise Factor	-	2.0		1.7		1.2		19.0		3.8		2.9		2.3		1.8		1.4		
Cascaded NF	[dB]	3.0		2.2		0.9		12.8		5.8		4.6		3.6		2.5		1.5		
Cascaded IIP3	[mW]	1.6		1.3		0.9		158.0		inf		inf		inf		inf		inf		
Cascaded IIP3	[dBm]	1.9		1.1		-0.3		22.0		50.4		49.7		52.6		52.4		60.0		

Fig. 2. Level plan of proposed white space converter.

range between 1 dB and 31 dB, the flexibility to optimize the prototype between NF and IIP3 is readily available. As a generic estimate for the parameters of a commercial WLAN router, a noise figure of 5 dB and an IIP3 of -12 dBm are considered [10], [11].

When the attenuator is at its lowest attenuation setting of 1 dB, the noise figure of the whole converter-router combination approaches its best value of 3 dB, but the linearity suffers as the gain of the whole link drives the receiver into saturation. Here, the IIP3 of the whole setup turns out to be -29 dBm, which is significantly worse than our intended target. Alternatively, when the attenuator is at its highest attenuation setting of 31 dB, the IIP3 shows an improved value of -1.9 dBm, but the NF of the whole setup worsens to 17.6 dB, which is unacceptable according to the standard. Thus, there exists a sweetspot where both the NF and the IIP3 are within acceptable limits as per definition of the standard. One optimum point in this region may be identified through the the Spurious Free Dynamic Range (SFDR) which is defined in [12] as

$$SFDR = \frac{2}{3}(P_{IIP3} - NF - 10\log(B) + 174) - SNR \quad (4)$$

The SFDR represents the range of levels of the desired signal over which it can be successfully received in the presence of any unwanted effects. Variations of the performance and dynamic range with the attenuator are presented in Fig. 3 and Fig. 4. As shown here, the maximum dynamic range is achieved when the attenuator in the WSC is set to 23 dB, resulting in a NF of 10.3 dB and a P_{IIP3} of around -8 dBm. However, in this setting, the NF is only within 1 dB to the theoretical acceptable value described in the standard and is thus deemed unsafe for real implementations. By slightly lowering the dynamic range through setting the attenuation to 20 dB, the NF of the converter is found to be 8 dB and the P_{IIP3} becomes -10.8 dBm. Hereby, both the NF and IIP3 are approximately 2 to 3 dB better than the minimum requirements and are also within our intended target values. Furthermore, this optimum SFDR of 48.5 dB is also close to the maximum achievable SFDR of 48.9 dB.

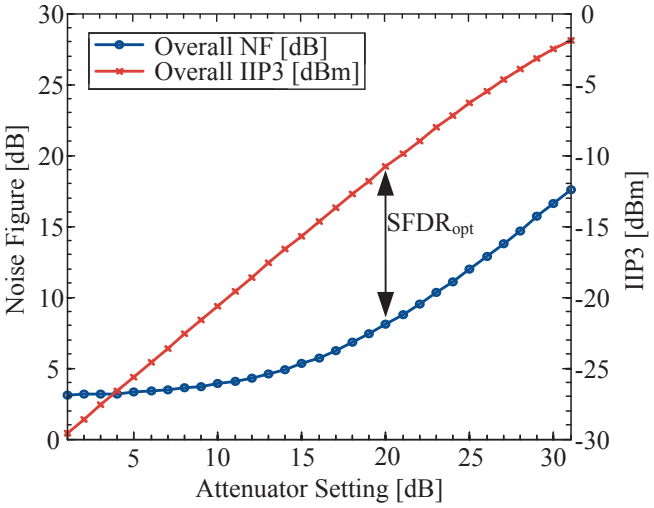

Fig. 3. Effect of Attenuator on Performance of the Converter-Router setup

It is also worthwile to mention that varying the attenuation settings alter only the noise figure and not the IIP3. Since the active devices in the converter chain (LNA and mixer) are more vulnerable to nonlinearities, the IIP3 of the converter is dominated by these blocks. Any gain reduction of the link through increasing the attenuation does not influence the IIP3 terms of the LNA and the mixer, i.e. the IIP3 of the converter remains unaffected by the attenuator settings. Consequently, this converter is not restricted in its usage to any specific WLAN device, but can be used as a bi-directional frequency translator for most commercial WLAN equipments.

C. Hardware Implementation

The prototype of the converter is depicted in Fig. 5. The hardware is implemented as a 4-layer PCB with the RF signals, ground plane, routing and digital signals forming the layer stackup. Care is taken to provide electromagnetic shielding to prevent a degradation in performance of the sensitive RF parts. The converter can be operated with a 12 V external supply. Level converters push the 12 V down to 5 V and then to the

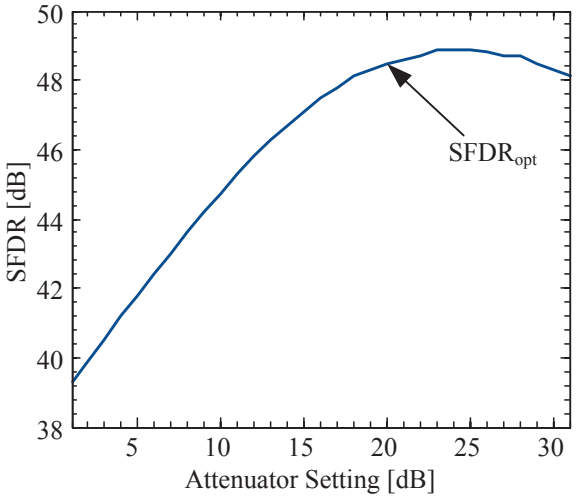

Fig. 4. Spurious Free Dynamic Range over Attenuator sweep

3.3 V domain which is the operating voltage of most of the component parts. The overall current consumption of the WSC is around 800 mA. The whole board occupies 90 mm x 56 mm.

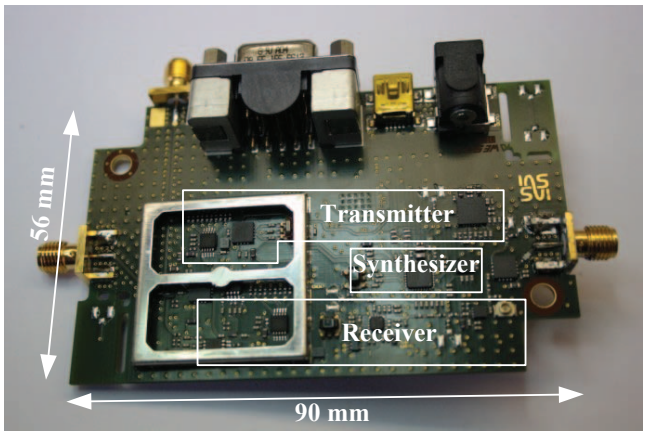

Fig. 5. Hardware of the white space converter prototype

V. Conclusions and Outlook

In this paper we have presented a novel bidirectional UHF-ISM band converter that enables legacy WLAN devices to operate over TV whitespaces. Our design is flexible, generic, and supports essential CR functionalities such as sensing and spectrum-agility. One of the main challenges in the design is to match the converter capabilities to the performance requirements of the IEEE 802.11 specifications. First theoretical studies show that a good tradeoff between noise figure and IIP3 power can be achieved, but that further research with our production quality prototype hardware is necessary. We have identified interference rejection from incumbent broadcasting networks as one of the main challenges for the converter design. The high fragmentation of channel usage that is apparent in today's TV broadcasting networks, especially in Europe, hampers whitespace operations due to the several orders of magnitude difference in transmit powers.

We have implemented the proposed architecture in a 4-layer PCB and are currently conducting first performance studies for different deployment scenarios and transceiver configurations. Once available, these characterization and measurements of the prototype will be made accessible through [13]. Besides further improvements on the usability side including an integrated cognitive engine for link parameters and a transition to USB powered operations, we envision to conduct further studies on the performance impact of various transmit/receive switching layouts.

Acknowledgements

The authors acknowledge the support of the Bundesministerium für Bildung und Forschung (BMBF), UMIC research cluster at RWTH Aachen University and the Deutsche Forschungsgemeinschaft (DFG). We also thank Prof. Petri Mähönen and Dr. Ljiljana Simić for their fruitful discussions.

References

[1] M. Wellens and P. Mähönen, "Lessons learned from an extensive spectrum occupancy measurement campaign and a stochastic duty cycle model," in *5th International Conference on Testbeds and Research Infrastructures for the Development of Networks Communities and Workshops (TridentCom)*, pp. 1–9, 2009.

[2] S. Haykin, "Cognitive radio: brain-empowered wireless communications," *IEEE Journal on Selected Areas in Communications*, vol. 23, no. 2, pp. 201–220, 2005.

[3] Federal Communications Commission, "In the matter of unlicensed operation in the TV broadcast bands: Second memorandum opinion and order," 2010.

[4] L. Simić, M. Petrova, and P. Mähönen, "Wi-Fi, but not on steroids: Performance analysis of a Wi-Fi-like network operating in TVWS under realistic conditions," in *to appear in Proc. ICC*, (Ottawa), 2012.

[5] S. Heinen and R. Wunderlich, "High dynamic range RF frontends from multiband multistandard to Cognitive Radio," in *Semiconductor Conference Dresden (SCD)*, pp. 1–8, Sep 2011.

[6] S. Narlanka, R. Chandra, P. Bahl, and J. Ferrell, "A Hardware Platform for Utilizing TV Bands With a Wi-Fi Radio," in *15th IEEE Workshop on Local Metropolitan Area Networks (LANMAN)*, pp. 49–53, 2007.

[7] IEEE SA, "IEEE 802.11b-1999 (R2003): Specific requirements - Part 11: Wireless LAN Medium Access Control (MAC) and Physical Layer (PHY) specifications: Higher-Speed Physical Layer Extension in the 2.4 GHz Band," tech. rep., IEEE, 2003.

[8] IEEE SA, "IEEE Std 802.11g-2003: Wireless LAN Medium Access Control (MAC) and Physical Layer (PHY) specifications: Further Higher Data Rate Extension in the 2.4 GHz Band," tech. rep., IEEE, 2003.

[9] J. Van De Beek, J. Riihijärvi, A. Achtzehn, and P. Mähönen, "UHF white space in Europe - A quantitative study into the potential of the 470-790 MHz band," in *IEEE Symposium on New Frontiers in Dynamic Spectrum Access Networks (DySPAN)*, pp. 1–9, 2011.

[10] L. Nathawad, D. Weber, S. Abdollahi, P. Chen, S. Enam, B. Kaczynski, A. Kheirkhahi, M. Lee, S. Limotyrakis, K. Onodera, K. Vleugels, M. Zargari, and B. Wooley, "An IEEE 802.11a/b/g SoC for Embedded WLAN Applications," in *IEEE International Solid-State Circuits Conference (ISSCC)*, pp. 1430–1439, 2006.

[11] A. Behzad *et al.*, "A Fully Integrated MIMO Multi-Band Direct-Conversion CMOS Transceiver for WLAN Applications (802.11n)," in *IEEE International Solid-State Circuits Conference (ISCC)*, pp. 560–622, 2007.

[12] B. Razavi, *RF Microelectronics*. Prentice-Hall, 1998.

[13] http://www.ias.rwth-aachen.de/whiteLAN.